

RESEARCH PAPER



Synthesis and biological evaluation of *N*-arylpiperazine derivatives of 4,4-dimethylisoquinoline-1,3(2*H*,4*H*)-dione as potential antiplatelet agents

Monika Marcinkowska^a, Magdalena Kotańska^b, Agnieszka Zagórska^a, Joanna Śniecikowska^a, Monika Kubacka^b, Agata Siwek^c, Adam Bucki^a, Maciej Pawłowski^a, Marek Bednarski^d, Jacek Sapa^d, Małgorzata Starek^e, Monika Dąbrowska^e and Marcin Kołaczkowski^a

^aDepartment of Medicinal Chemistry, Jagiellonian University Medical College, Kraków, Poland; ^bDepartment of Pharmacological Screening, Chair of Pharmacodynamics, Jagiellonian University Medical College, Kraków, Poland; ^cDepartment of Pharmacobiology, Jagiellonian University Medical College, Kraków, Poland; ^dDepartment of Pharmacological Screening, Chair of Pharmacodynamics, Jagiellonian University Medical College, Kraków, Poland; ^eDepartment of Inorganic and Analytical Chemistry, Faculty of Pharmacy, Jagiellonian University Medical College, Kraków, Poland

ABSTRACT

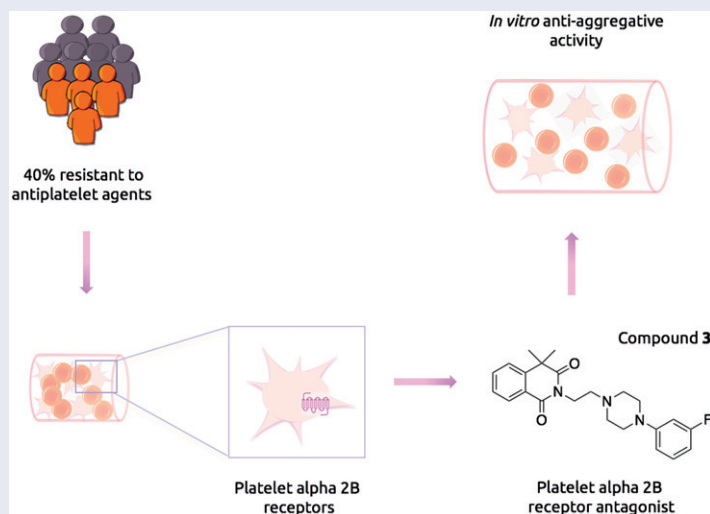
Despite the substantial clinical success of aspirin and clopidogrel in secondary prevention of ischemic stroke, up to 40% of patients remain resistant to the available antiplatelet treatment. Therefore, there is an urgent clinical need to develop novel antiplatelet agents with a novel mechanism of action. Recent studies revealed that potent alpha 2B-adrenergic receptor (alpha 2B-ARs) antagonists could constitute alternative antiplatelet therapy. We have synthesized a series of *N*-arylpiperazine derivatives of 4,4-dimethylisoquinoline-1,3(2*H*,4*H*)-dione as potential alpha 2B receptor antagonists. The most potent compound **3**, effectively inhibited the platelet-aggregation induced both by collagen and ADP/adrenaline with IC₅₀ of 26.9 μM and 20.5 μM respectively. Our study confirmed that the alpha 2B-AR antagonists remain an interesting target for the development of novel antiplatelet agents with an alternative mechanism of action.

ARTICLE HISTORY

Received 27 July 2017
Revised 18 January 2018
Accepted 1 February 2018

KEYWORDS

Antiplatelet agents;
blockade of the platelet
aggregation; alpha 2B
receptor antagonists;
ARC-239



Introduction

Antiplatelet drugs are the mainstay of the pharmacological treatment for patients with various cardiovascular diseases¹. Large clinical trials have revealed that treatment with antiplatelet agents such as clopidogrel and aspirin may reduce the risk of myocardial infarction, stroke or death by almost 22%². This fact has made them one of the most widely prescribed drugs in the world³.

However, despite significant clinical success in preventing the adverse outcome of cardiovascular diseases, many patients experience recurrent atherothrombotic events, despite the treatment with antiplatelet agents. Moreover, many patients are resistant to aspirin and/or clopidogrel, which results in poor prognosis and increased risk of further cardiovascular events².

Clopidogrel and aspirin act via a blockade of adenosine diphosphate (ADP) receptor and inhibition of cyclooxygenase-1 (COX-1)

CONTACT Monika Marcinkowska ✉ monika.marcinkowska@uj.edu.pl Department of Medicinal Chemistry, Jagiellonian University Medical College, 9 Medyczna Street, Kraków 30-688, Poland

© 2018 The Author(s). Published by Informa UK Limited, trading as Taylor & Francis Group.

This is an Open Access article distributed under the terms of the Creative Commons Attribution License (<http://creativecommons.org/licenses/by/4.0/>), which permits unrestricted use, distribution, and reproduction in any medium, provided the original work is properly cited.

respectively. These mechanisms result in the inhibition of the platelet activation and aggregation and further clot formation⁴. It has been suggested that aspirin resistance may be related to the lack or insufficient inhibition of the COX-1-mediated thromboxane A2 pathway, while clopidogrel resistance is related to the P2Y12 ADP receptor signaling^{5,6}. Therefore, there is an urgent clinical need to develop novel antiplatelet agents involving different pathways of platelet aggregation, which would constitute an alternative for the treatment of resistant patients.

Recent studies revealed that the blockade of platelet alpha 2B-adrenergic receptors (alpha 2B-ARs) may play a role in platelet aggregation^{7,8}. Interestingly, inhibition of alpha 2B-ARs in patients with ischemic heart disease, treated with clopidogrel and aspirin, resulted in an additional antiplatelet effect⁹. Moreover, it has been shown that adrenaline under the stimulation of alpha-adrenergic receptors leads to increased platelet aggregation and may overcome the aspirin-induced blockade of platelet function^{10,11}. Therefore, the blockade of platelet alpha 2B-ARs may have also a clinical benefit for aspirin-resistant patients. The results of these studies suggest that the blockade of platelet alpha 2B-ARs offers a new therapeutic strategy for the development of novel antiplatelet agents.

Among many structurally different classes of alpha adrenergic ligands, arylpiperazine derivatives have been the most intensively investigated¹². The conformationally rigid arylpiperazine fragment is crucial for proper interactions with the alpha 2B-AR. It provides charge-reinforced hydrogen bond between nitrogen atom of piperazine ring and Asp3.32 residue from the orthosteric binding site of alpha 2B-ARs. At the same time, the phenyl ring enables essential aromatic CH- π stacking with Phe6.52, which provides further stabilization of the ligand-receptor complex, along with interactions in the second (allosteric) binding site (Figure 2)^{13,14}.

A phenylpiperazine derivative of 4,4-dimethylisoquinoline-1,3(2H,4H)-dione, compound ARC-239 (Figure 1), is a well-known, potent alpha 2B receptor antagonist, selective vs. 2A subtype¹⁵. However, as an *ortho*-methoxyphenylpiperazine derivative, ARC-239 shares a similar pharmacophore with alpha 1 adrenoceptor ligands¹². In fact, our research, in addition to other literature reports, show that ARC-239 exhibits strong binding affinity also for alpha 1 adrenoceptor (Table 1)^{12,16}, which could be the source of additional unwanted adverse reactions¹⁷. We used the compound ARC-239 as a starting point in the design of selective alpha 2B-AR ligands with antiplatelet activity, assuming that it can be deprived of the alpha 1 adrenergic activity, by changing the substitution pattern at the phenylpiperazine moiety. It has been

reported that *ortho*-methoxyphenyl group is privileged for alpha 1A receptor affinity^{18,19}. Therefore, in order to obtain selective alpha 2B-AR ligands, we replaced the *ortho*-methoxyphenyl group with meta-substituted phenyl moiety or with bulkier hetero-aromatic rings, all acceptable for alpha 2B-AR binding site restrictions, while maintaining the 4,4-dimethylisoquinoline-1,3(2H,4H)-dione scaffold unchanged (Figure 1). The latter moiety has been recognized as a key pharmacophore fragment and therefore its replacement might result in loss of affinity or selectivity towards alpha adrenergic receptors²⁰. Therefore, we postulated that modifications restricted to the phenylpiperazine scaffold would reduce the interaction with alpha 1-AR while maintaining the alpha 2-AR affinity.

Moreover, previous research showed that bulky aromatic substituents rich in π electrons may increase the electrostatic interactions with aromatic amino acid residues of alpha 2-AR binding pocket^{21,22}. Therefore, by enhancing the electron density with a proper aromatic substituent, we expected to strengthen interactions between the aromatic ring and Phe6.52 residue of alpha 2-AR binding pocket and thus increase ligand affinity for this molecular target.

Furthermore, in order to avoid interaction with other monoaminergic receptors (e.g. serotonin 5-HT1A, 5-HT2A, and dopamine D2), we kept the original ethyl chain, linking the phenylpiperazine fragment and 4,4-dimethylisoquinoline-1,3(2H,4H)-dione. It is worth mentioning that previously it has been shown that increasing the length of an alkyl linker in phenylpiperazine derivatives might result in increased affinity towards the above-mentioned undesirable receptor targets^{23,24}.

The proposed binding mode of the designed compounds, presented on the example of the prototype compound **4**, shows

Table 1. Molecular properties and PAINS analysis.

Compound	Lipinski rule of 5				Veber filter		PAINS #Alerts
	QLogP	MW	HBD	HBA	RB	TPSA	
3	4.1	395.5	0	6	3	55.3	0
4	4.4	411.9	0	6	3	55.4	0
5	5.0	445.5	0	6	3	59.7	0
6	3.9	407.5	0	7	4	63.6	0
7	3.3	393.5	1	7	4	78.0	0
8	2.7	379.5	0	8	3	73.9	0
9	4.1	449.5	0	8	3	70.6	0
10	2.4	434.5	1	9	3	109.3	0
11	2.8	448.5	1	9	3	104.6	0

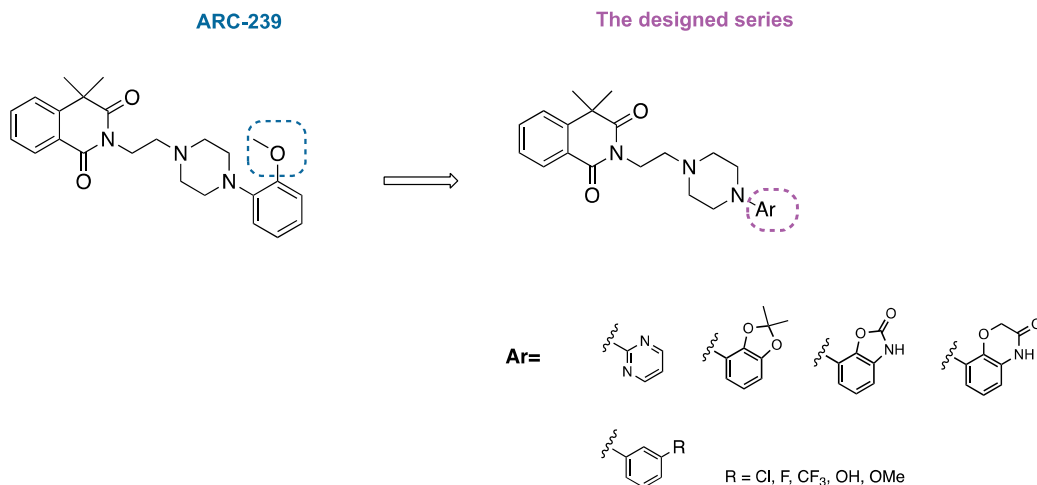


Figure 1. Structures of the designed 4,4-dimethylisoquinoline-1,3(2H,4H)-dione derivatives.

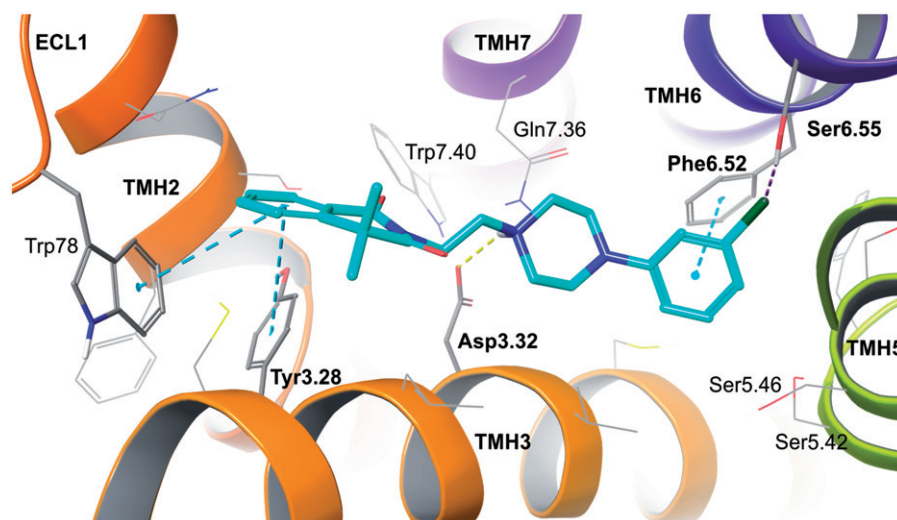


Figure 2. Prototype compound 4 in alpha 2B adrenergic receptor homology model based on beta 2 adrenergic receptor crystal structure (2RH1). Amino acid residues engaged in ligand binding (within 4 Å from the ligand atoms) are displayed as sticks, whereas those forming typical H-bonds (dotted yellow lines), π - π stacking (dotted blue lines) or H-bonds to halogens (dotted purple line) are represented as thick sticks. The extracellular loop (ECL) 2 was hidden for clarity. TMH – transmembrane helix.

well-recognized anchoring interactions of arylpiperazine fragment in the orthosteric binding site, between transmembrane helices (TMHs) 3, 5, and 6^{25,26}. Those include charge-reinforced hydrogen bond of protonated piperazine with Asp3.32 and π - π stacking of 3-chlorophenyl ring with Phe6.52, additionally stabilized by weak interaction of chlorine substituent with Ser6.55. The standard interactions for monoaminergic receptor ligands are complemented by 4,4-dimethylisoquinoline-1,3(2*H*,4*H*)-dione aromatic bonds (π - π stacking) with residues from the second (allosteric) binding site. These are Tyr3.28 from TMH3 and Trp78 from extracellular loop (ECL) 1 (Figure 2).

Materials and methods

Molecular modeling

Ligand docking studies involved human adrenergic alpha 2B receptor homology model, developed using the well-validated method²⁷.

The novel homology model was built on the basis of adrenergic β_2 receptor crystal structure (PDB ID: 2RH1)²⁸. Sequence alignment between target receptor (UniProt database accession number P18089) and the template were performed by hhsearch tool via GeneSilico Metaserver (<https://www.genesilico.pl/meta2/>)²⁹. The artificial fragments replacing the third intracellular loop (ICL3) in the protein crystal structure were removed and short loops were created. The crude receptor models were obtained using SwissModel (<https://swissmodel.expasy.org/>)³⁰ and were validated by processing in Protein Preparation Wizard. ARC-239 structure was utilized for ligand-based binding site optimization, performed using induced fit docking (IFD) workflow. That procedure resulted in conformational receptor model that served as molecular target in docking studies.

Ligand structures were optimized using LigPrep tool (Schrödinger, LLC, New York, USA). Glide SP flexible docking procedure was carried out using default parameters. OPLS3 force field was applied on both energy minimization (protein and ligands) and docking stages. H-bond constraint, as well as centroid of a grid box for docking studies were located on Asp3.32.

Molecular properties were calculated using QikProp software (Schrödinger, LLC, New York, USA) (QLogP – Predicted octanol/

water partition coefficient; MW – molecular weight; HBD – hydrogen bond donor; HBA – hydrogen bond acceptor; RB – rotatable bonds; TPSA – total polar surface area). Number of PAINS alerts determined by SwissADME server (www.swissadme.ch)³¹, ADME parameters were predicted by: QikProp (QLogS – solubility; QPPCaco – Caco-2 cell permeability; % PO Absorption – percent human oral absorption), SwissADME (BBB – blood-brain barrier permeability; Pgp – substrate of glycoprotein P) and VolSurf+ version 1.0.7.1 from Molecular Discovery (Borehamwood, UK) (PB – % of protein binding; MetStab – metabolic stability after CYP incubation).

Glide, induced fit docking, LigPrep, Protein Preparation Wizard, and QikProp were implemented in Small-Molecule Drug Discovery Suite (Schrödinger Release 2017–1: Maestro, Schrödinger, LLC, New York, NY, USA, 2017), which was licensed for Jagiellonian University Medical College.

Chemistry

Unless otherwise indicated, all the starting materials and the reference compound ARC-239 were obtained from commercial suppliers and were used without further purification. Analytical thin-layer chromatography (TLC) was performed on Merck Kieselgel 60 F₂₅₄ (0.25 mm) pre-coated aluminum sheets (Merck, Darmstadt, Germany). Visualization was performed with a 254 nm UV lamp. Column chromatography was performed using silica gel (particle size 0.063–0.200 mm; 70–230 Mesh ATM) purchased from Merck. The UPLC-MS or UPLC-MS/MS analyses were run on UPLC-MS/MS system comprising Waters ACQUITY® UPLC® (Waters Corporation, Milford, MA, USA) coupled with Waters TQD mass spectrometer (electrospray ionization mode ESI with tandem quadrupole). Chromatographic separations were carried out using the ACQUITY UPLC BEH (bridged ethyl hybrid) C₁₈ column: 2.1 × 100 mm and 1.7 μ m particle size. The column was maintained at 40 °C and eluted under gradient conditions using 95% to 0% of eluent A over 10 min, at a flow rate of 0.3 ml/min. Eluent A: water/formic acid (0.1%, v/v); eluent B: acetonitrile/formic acid (0.1%, v/v). A total of 10 μ l of each sample were injected, and chromatograms were recorded using Waters eλ PDA detector. The spectra were analyzed in the range of 200–700 nm with 1.2 nm resolution and at a sampling rate of 20 points/s. MS detection

settings of Waters TQD mass spectrometer were as follows: source temperature 150 °C, desolvation temperature 350 °C, desolvation gas flow rate 600 l/h, cone gas flow 100 l/h, capillary potential 3.00 kV, and cone potential 20 V. Nitrogen was used for both nebulizing and drying. The data were obtained in a scan mode ranging from 50 to 1000 *m/z* at 0.5 s intervals; 8 scans were summed up to obtain the final spectrum. Collision activated dissociation (CAD) analyses were carried out with the energy of 20 eV, and all the fragmentations were observed in the source. Consequently, the ion spectra were obtained in the range from 50 to 500 *m/z*. MassLynx V 4.1 software (Waters) was used for data acquisition. Standard solutions (1 mg/ml) of each compound were prepared in a mixture comprising analytical grade acetonitrile/water (1/1, v/v). The UPLC/MS purity of all the test compounds and key intermediates was determined to be >95%. ¹H NMR and ¹³C NMR spectra were obtained in a Varian Mercury spectrometer (Varian Inc., Palo Alto, CA, USA), in CDCl₃, operating at 300 MHz (¹H NMR), 75 MHz (¹³C NMR). Chemical shifts are reported in terms of δ values (ppm) relative to TMS $\delta = 0$ (¹H) as internal standard. The *J* values are expressed in Hertz. Signal multiplicities are represented by the following abbreviations: s (singlet), br.s (broad singlet), d (doublet), dd (doublet of doublets), t (triplet), q (quartet), m (multiplet). Elemental analysis was performed using the VarioEL III – Elementar apparatus (Hanau, Germany).

General procedure for the synthesis of 2-(2-chloroethyl)-4,4-dimethylisoquinoline-1,3(2H,4H)-dione (2)

A mixture of 4,4-dimethylisoquinoline-1,3(2H,4H)-dione (2.11 mmol), 1-bromo-2-chloroethane (5.58 mmol), potassium carbonate (8.68 mmol), trimethylamine (3.96 mmol) in acetone (20 ml) was stirred for 72 h at 55 °C. Next, the reaction mixture was cooled to the room temperature, potassium carbonate was filtered off and the solvent was evaporated under the reduced pressure. The crude mixture was purified via column chromatography using n-hexane:DCM:MeOH 40:59.6:0.5 (v/v) as eluent.

Yield 60%, yellow crystallizing oil, ¹H NMR (300 MHz, CDCl₃): δ 8.24–8.18 (m, 1H), 7.67–7.60 (m, 1H), 7.48–7.38 (m, 2H), 4.39–4.33 (t, *J* = 6.6 Hz, 2H), 3.76–3.70 (t, *J* = 6.6 Hz, 2H), 1.63 (s, 6H); Formula: C₁₃H₁₄ClNO₂; ESI-MS: 252 [M + H]⁺.

General procedure for the synthesis of the final molecules (3–11)

Method C (for compounds 3–6)

A mixture of 2-(2-chloroethyl)-4,4-dimethylisoquinoline-1,3(2H,4H)-dione (2) (0.247 mmol) and corresponding piperazine (0.5 mmol) was stirred at 140 °C for 30 min. After this time, the reaction mixture was cooled to room temperature, EtOAc (4 ml) was added, and the resulted solid was filtered off. The remaining solution was concentrated in vacuum and further purified via column chromatography using n-hexane:Et₂O:DCM 20:40:40 or DCM:EtOAc:MeOH 69.8:30:0.2 as eluent.

2-(2-(4-(3-Fluorophenyl)piperazin-1-yl)ethyl)-4,4-dimethylisoquinoline-1,3(2H,4H)-dione (3)

Yield 41%, pale yellow oil, ¹H NMR (300 MHz, CDCl₃): δ 8.24–8.20 (dd, *J* = 1.0 and 7.7 Hz, 1H), 7.68–7.60 (m, 1H), 7.49–7.38 (m, 2H), 7.17–7.10 (t, *J* = 7.9 Hz, 1H), 6.86–6.72 (m, 3H), 4.24–4.17 (t, *J* = 6.6 Hz, 2H), 3.16–3.08 (t, *J* = 4.9 Hz, 4H), 2.70–2.62 (m, 6H), 1.63 (s, 6H); ¹³C NMR (75 MHz, CDCl₃): δ : 177.1, 164.1, 163.8, 152.1, 145.1, 135.2, 129.7, 128.3, 127.3, 127.2, 125.1, 118.7, 115.6, 111.8,

55.6, 53.4 (2C), 48.6 (2C), 43.6, 37.1, 29.4 (2C); Formula: C₂₃H₂₆FN₃O₂; ESI-MS: 396 [M + H]⁺.

2-(2-(4-(3-Chlorophenyl)piperazin-1-yl)ethyl)-4,4-dimethylisoquinoline-1,3(2H,4H)-dione (4)

Yield 38%, pale yellow oil, ¹H NMR (300 MHz, CDCl₃): δ 8.24–8.20 (dd, *J* = 1.0 and 7.7 Hz, 1H), 7.68–7.60 (m, 1H), 7.49–7.38 (m, 2H), 7.17–7.10 (t, *J* = 7.9 Hz, 1H), 6.86–6.72 (m, 3H), 4.24–4.17 (t, *J* = 6.6 Hz, 2H), 3.16–3.08 (t, *J* = 4.9 Hz, 4H), 2.70–2.62 (m, 6H), 1.63 (s, 6H); ¹³C NMR (75 MHz, CDCl₃): δ 177.0, 164.1, 152.0, 145.0, 135.3, 129.2, 128.5, 127.3, 126.3, 125.6, 123.8, 118.3, 114.6, 111.2, 55.4, 53.3 (2C), 48.8 (2C), 43.4, 37.2, 29.3 (2C); Formula: C₂₃H₂₆ClN₃O₂; ESI-MS: 412 [M + H]⁺.

4,4-Dimethyl-2-(2-(4-(3-(trifluoromethyl)phenyl)piperazin-1-yl)ethyl)isoquinoline-1,3(2H,4H)-dione (5)

Yield 35%, pale yellow oil, ¹H NMR (300 MHz, CDCl₃): δ 8.24–8.20 (dd, *J* = 1.0 and 7.9 Hz, 1H), 7.67–7.59 (m, 1H), 7.48–7.39 (m, 2H), 7.35–7.22 (t, *J* = 8.2 Hz, 1H), 7.09–6.98 (m, 3H), 4.25–4.15 (t, *J* = 6.6 Hz, 2H), 3.20–3.10 (t, *J* = 4.9 Hz, 4H), 2.72–2.64 (m, 6H), 1.63 (s, 6H); ¹³C NMR (75 MHz, CDCl₃): δ 177.1, 164.1, 151.3, 145.0, 133.9, 131.6 (q, *J* = 63.0 and 31.5 Hz), 129.4, 128.8, 127.3, 126.2, 125.1, 123.8, 118.5, 115.5, 111.8, 55.5, 53.4 (2C), 48.6 (2C), 43.5, 37.2, 29.4 (2C); Formula: C₂₄H₂₆F₃N₃O₂; ESI-MS: 446 [M + H]⁺.

2-(2-(4-(3-Methoxyphenyl)piperazin-1-yl)ethyl)-4,4-dimethylisoquinoline-1,3(2H,4H)-dione (6)

Yield 61%, yellow oil, ¹H NMR (300 MHz, CDCl₃): δ 8.26–8.18 (dd, *J* = 0.7 and 7.7 Hz, 1H), 7.66–7.58 (m, 1H), 7.48–7.38 (m, 2H), 7.18–7.10 (t, *J* = 7.9 Hz, 1H), 6.54–6.48 (m, 1H), 6.46–6.36 (m, 2H), 4.24–4.18 (t, *J* = 6.6 Hz, 2H) 3.78 (s, 3H), 3.16–3.08 (t, *J* = 4.61 Hz, 4H), 2.72–2.62 (m, 6H) 1.63 (s, 6H); ¹³C NMR (75 MHz, CDCl₃): δ 177.0, 164.1, 160.5, 152.7, 145.0, 133.9, 129.7, 128.8, 127.2, 125.0, 123.9, 108.6, 104.2, 102.2, 55.5, 55.1, 53.2 (2C), 49.0 (2C), 43.5, 37.2, 29.3 (2C); Formula: C₂₄H₂₉N₃O₃; ESI-MS: 408 [M + H]⁺.

General procedure for the synthesis of 2-(2-(4-(3-hydroxyphenyl)piperazin-1-yl)ethyl)-4,4-dimethylisoquinoline-1,3(2H,4H)-dione (7)

To a solution of 2-(2-(4-(3-methoxyphenyl)piperazin-1-yl)ethyl)-4,4-dimethylisoquinoline-1,3(2H,4H)-dione (6) (0.312 mmol) in 5 ml of DCM, at 0 °C BBr₃ (0.624 mmol) was added dropwise. The resulted orange slurry was stirred for 24 h at room temperature. After that time, methanol (10 ml) was added and the reaction mixture was quenched with water. Next, the organic layer was washed with water, dried over sodium sulfate and the solvent was evaporated. The crude mixture was purified via column chromatography using n-hexane:EtOAc:DCM:MeOH 10:10:79.8:0.2 as eluent.

Yield 75%, brown oil, ¹H NMR (300 MHz, CDCl₃): δ 8.25–8.19 (dd, 1H, *J* = 1.0 and 7.7 Hz), 7.66–7.59 (m, 1H), 7.49–7.35 (m, 2H), 7.08–6.98 (m, 1H), 6.49–6.40 (m, 1H), 6.35–6.25 (m, 2H), 5.2 (s, 1H), 4.25–4.19 (t, 2H, *J* = 6.6 Hz), 3.05–3.12 (t, 4H, *J* = 4.4 Hz), 2.74–2.65 (m, 6H), 1.63 (s, 6H); ¹³C NMR (75 MHz, CDCl₃): δ 177.2, 164.2, 152.6, 145.1, 135.8, 133.9, 129.9, 128.9, 127.3, 125.1, 124.7, 108.2, 106.8, 103.1, 55.5, 53.1 (2C), 48.8 (2C), 43.6, 37.2, 29.3 (2C); Formula: C₂₃H₂₇N₃O₃; ESI-MS: 394 [M + H]⁺.

General procedure for the synthesis of the final molecules (8–10)

Method B (for compounds 8–10)

A mixture of 2-(2-chloroethyl)-4,4-dimethylisoquinoline-1,3(2*H*,4*H*)-dione (**2**) (0.247 mmol) and corresponding piperazine (0.5 mmol) was stirred at 140 °C for 30 min. After this time, the reaction mixture was cooled to room temperature, EtOAc (4 ml) was added, and the resulted solid was filtered off. The crude mixture was purified via column chromatography using n-hexane:Et₂O:DCM 20:40:40 or DCM:EtOAc:MeOH 69.8:30:0.2 as eluent.

4,4-Dimethyl-2-(2-(4-(pyrimidin-2-yl)piperazin-1-yl)ethyl)isoquinoline-1,3(2*H*,4*H*)-dione (**8**)

Yield 30%, dark yellow oil, ¹H NMR (300 MHz, CDCl₃): δ 8.26–8.18 (dd, *J* = 0.7 and 7.7 Hz, 1H), 7.63–7.60 (m, 1H), 7.48–7.39 (m, 2H), 7.09–6.99 (m, 2H), 6.48–6.44 (m, 1H), 4.25–4.18 (t, *J* = 6.6 Hz, 2H) 3.77, 3.16–3.07 (t, *J* = 4.6 Hz, 4H), 2.73–2.61 (m, 6H) 1.63 (s, 6H); ¹³C NMR (75 MHz, CDCl₃): δ 178.1, 165.0, 147.8, 145.0, 135.1, 134.2, 129.0, 127.4, 125.1, 124.7, 123.5, 121.1, 61.7 (2C), 43.7 (2C), 42.9, 34.2, 30.1, 29.3 (2C) Formula: C₂₁H₂₅N₅O₂; ESI-MS: 380 [M + H]⁺.

2-(2-(4-(2,2-Dimethylbenzo[d][1,3]dioxol-4-yl)piperazin-1-yl)ethyl)-4,4-dimethylisoquinoline-1,3(2*H*,4*H*)-dione (**9**)

Yield 39%, pale yellow oil, ¹H NMR (300 MHz, CDCl₃): δ 8.25–8.18 (dd, *J* = 0.7 and 7.7 Hz, 1H) 7.66–7.58 (m, 1H), 7.48–7.39 (m, 2H), 6.74–6.66 (t, *J* = 7.9 Hz, 1H), 6.44–6.33 (m, 2H), 4.25–4.15 (t, *J* = 6.4 Hz, 2H), 3.17–3.08 (m, 4H), 2.75–2.61 (m, 6H), 1.68 (s, 6H), 1.66 (s, 6H); Formula: C₂₆H₃₁N₃O₄; Anal. calcd for C₂₆H₃₁N₃O₄: C, 69.47; H, 6.95; N, 9.35; Found: C, 69.25; H, 6.99; N, 9.38; ESI-MS: 450 [M + H]⁺.

4,4-Dimethyl-2-(2-(4-(2-oxo-3,4-dihydrobenzo[d]oxazol-7-yl)piperazin-1-yl)ethyl)isoquinoline-1,3(2*H*,4*H*)-dione (**10**)

Yield 33%, yellow oil, ¹H NMR (300 MHz, CDCl₃): δ 8.26–8.19 (dd, *J* = 0.7 and 7.6 Hz, 1H) 7.67–7.59 (m, 1H), 7.50–7.33 (m, 3H), 7.08–6.96 (m, 1H), 6.64–6.54 (m, 2H), 4.24–4.18 (t, *J* = 6.6 Hz, 2H), 3.30–3.20 (t, *J* = 4.3 Hz, 4H), 2.78–2.67 (m, 6H), 1.63 (s, 6H); Formula: C₂₄H₂₆N₄O₄; Anal. calcd for C₂₄H₂₆N₄O₄: C, 66.34; H, 6.03; N, 12.89; Found: C, 66.28; H, 6.07; N, 12.94; ESI-MS: 435 [M + H]⁺.

4,4-Dimethyl-2-(2-(4-(3-oxo-3,4-dihydro-2*H*-benzo[b][1,4]oxazin-8-yl)piperazin-1-yl)ethyl)isoquinoline-1,3(2*H*,4*H*)-dione (**11**)

Yield 67%, yellow oil, ¹H NMR (300 MHz, CDCl₃): δ 8.26–8.19 (dd, *J* = 0.7 and 7.7 Hz, 1H) 7.66–7.59 (m, 1H), 7.49–7.35 (m, 2H), 7.00–6.98 (m, 1H), 6.90–6.83 (t, *J* = 8.2 Hz, 1H), 6.62–6.58 (dd, *J* = 2.3 and 6.9 Hz, 1H), 6.45–6.49 (d, *J* = 7.6 Hz, 1H), 4.60 (s, 2H), 4.25–4.19 (t, *J* = 6.6 Hz, 2H), 3.08–3.00 (m, 4H), 2.78–2.64 (m, 6H), 1.63 (s, 6H); Formula: C₂₃H₂₂N₄O₄; Anal. calcd for C₂₃H₂₂N₄O₄: C, 66.95; H, 6.29; N, 12.49; Found: C, 66.87; H, 6.30; N, 12.52; ESI-MS: 449 [M + H]⁺.

Determination of the intrinsic activity of the test compounds at the α₂A-adrenoreceptors and α₂B-adrenoreceptors

An intrinsic activity assay was performed according to the instructions of the manufacturer of the assay kit containing ready-to-use cells with stable expression of the α₂A-adrenoceptor (In-vitrogen, Life Technologies, Carlsbad, CA, USA) or α₂B-adrenoceptor (PerkinElmer, Inc, Waltham, MA, USA).

Determination of the affinity of the test compounds at the α₁-adrenoreceptors and α₂-adrenoreceptors

The affinity of the obtained compounds was evaluated by radioligand binding assays (the ability to displace [³H] prazosin and [³H]clonidine from α₁- and α₂-AR, respectively) on rat cerebral cortex. The brains are homogenised in 20 volumes of an ice-cold 50 mM Tris-HCl buffer (pH 7.6) and is centrifuged at 20,000 g for 20 min (0–4 °C). The cell pellet is resuspended in the Tris-HCl buffer and centrifuged again. Radioligand binding assays are performed in plates (MultiScreen/Millipore). The final incubation mixture (final volume 300 μL) consisted of 240 μL of the membrane suspension, 30 μL of [³H]prazosin (0.2 nM) or [³H]clonidine (2 nM) solution and 30 μL of the buffer containing seven to eight concentrations (1.0^{−11} to 1.0^{−4} M) of the tested compounds. For measuring the unspecific binding, phentolamine, 10 μM (in the case of [³H]prazosin) and clonidine, 10 μM (in the case of [³H]clonidine) are applied. The incubation is terminated by rapid filtration over glass fiber filters (Whatman GF/C) using a vacuum manifold (Millipore). The filters are then washed twice with the assay buffer and placed in scintillation vials with a liquid scintillation cocktail. Radioactivity was measured in a WALLAC 1409 DSA liquid scintillation counter. All the assays were performed in duplicate.

In vitro whole blood aggregation test

In vitro aggregation tests were conducted using freshly collected whole blood with Multiplate platelet function analyzer (Roche Diagnostics Polska Sp. z o.o., Warsaw, Poland), the five-channel aggregometer based on measurements of electric impedance. The Multiplate analyzer allows the duplicate measurement with dual electrode probes. Blood was drawn from carotid of rats with hirudin blood tube (Roche Diagnostic). 300 μL of hirudin anticoagulated blood was mixed with 300 μL pre-warmed isotonic saline solution containing studied compound in DMSO or DMSO (0.1% final) and pre-incubated for 3 min at 37 °C with continuous stirring. The agonists (ADPtest, COLtest, Roche Diagnostic) were diluted using isotonic sterile NaCl solution. Aggregation was induced by adding collagen (final concentration 1.6 μg/mL), or adrenaline and subthreshold concentration of ADP (final concentration 50 μM + 1.6 μM). Activated platelet function was recorded for 6 min. The Multiplate software analyzed the area under the curve of the clotting process of each measurement and calculated the mean values.

Data were presented as Mean ± SEM. Statistical comparisons were made by the analysis of variance (ANOVA) and significance of the differences between control group and treated groups was determined by Dunnett *post hoc* test. *p* < .05 was considered significant.

The bioavailability assays

The *in vitro* bioavailability assays were performed by Eurofins Panlabs Inc. (St Charles, USA) according to the methods reported in publications listed below:

Solubility: Lipinski, C.A et al. (2001) Adv Drug Del Rev, 46:3–26³²,

Protein binding: Banker, M.J et al. (2003) J. Pharm. Sci., 92:967–974³³,

Caco-2 permeability: Hidalgo, I.J et al. (1989) Gastroenterology, 96:736–749³⁴,

Microsomal stability: Obach, R.S et al. (1997) J Pharmacol Exp Ther, 283:4658³⁵.

Results and discussion

Chemistry

The synthesis of a series of *N*-arylpiperazine derivatives of 4,4-dimethylisoquinoline-1,3(2*H*,4*H*)-dione (**3–11**) is presented in the Scheme 1. In the first step, alkylation of commercially available 4,4-dimethylisoquinoline-1,3(2*H*,4*H*)-dione (**1**) with 1-chloro-2-bromoethane in the presence of potassium carbonate and triethylamine yielded 2-(2-chloroethyl)-4,4-dimethylisoquinoline-1,3(2*H*,4*H*)-dione (**2**). The intermediate (**2**) was next reacted with corresponding arylpiperazines to give the final compounds **3–11**. Initially, we obtained the final molecules **3–11** with relatively small insufficient yields (8–15%), which was related to the parallel formation of the side product (**2a**). Therefore, we optimized the reaction conditions, changing the solvent from acetonitrile to dry dioxane, which allowed us to obtain the final products **8–11** with higher yields (30–67%, Method b, Scheme 1). Compounds **3–6** were obtained in solvent-free conditions, reacting the intermediate (**2**) with an excess of corresponding arylpiperazines (Method c, Scheme 1), which afforded the final compounds **3–6** with satisfactory yields (35–67%). Additionally, compound **7** was obtained via demethylation of corresponding methoxy derivative **6**, using BBr₃ in DCM at 0 °C.

Molecular properties and predicted ADME parameters

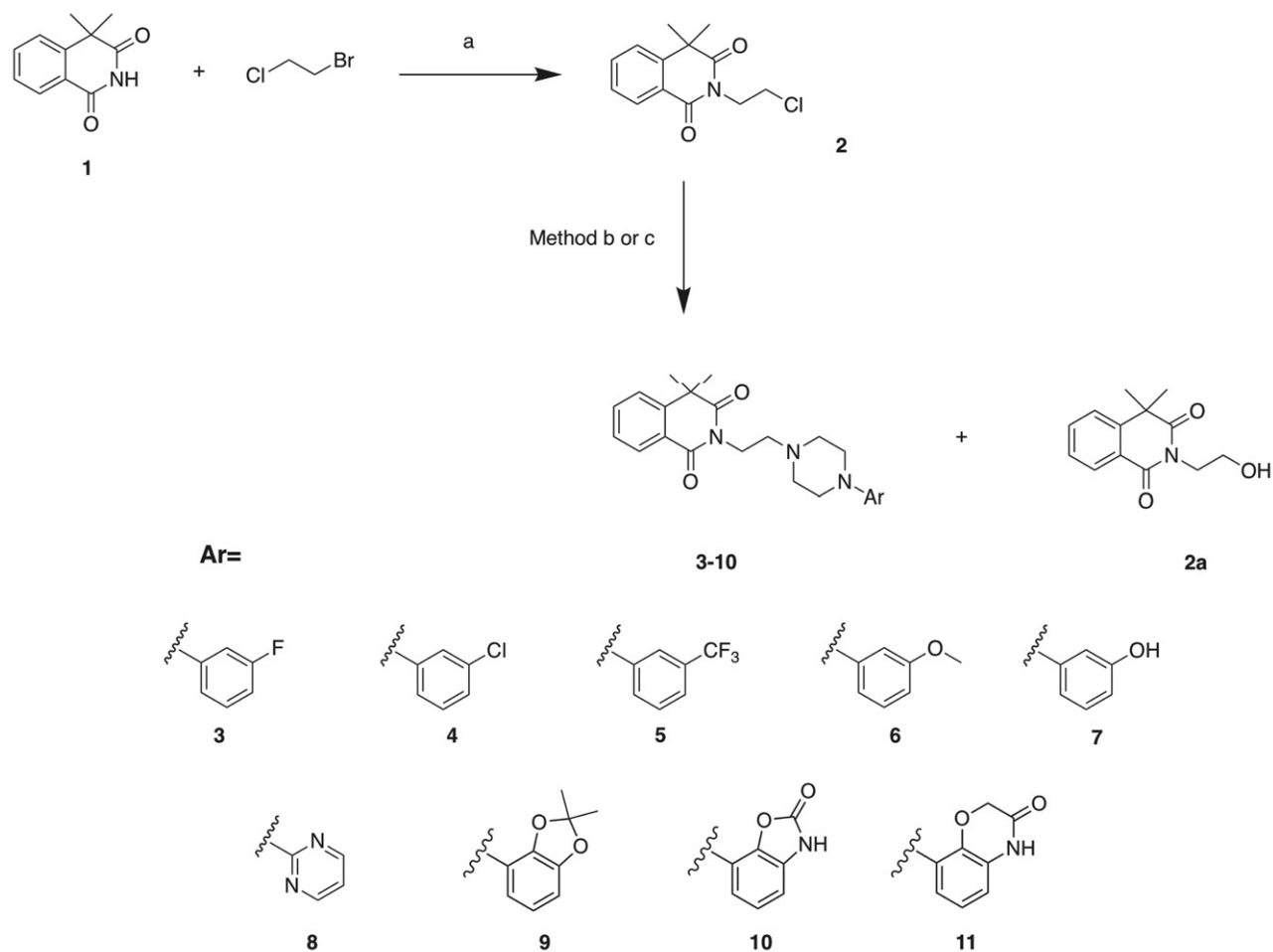
The newly designed structures were tested for compliance with two rules determining drug-like properties. Lipinski rule of five

and Veber filter evaluate bioavailability of a compound after oral administration. The first one assumes that compounds having LogPo/w (octanol/water partition coefficient) lower than 5, MW (molecular weight) below 500, less than 10 HBA (H-bond acceptors), and 5 HBD (H-bond donors) are more likely to show favorable bioavailability³². The Veber rule extends range of parameters with <10 rotatable bonds and TPSA (total polar surface area) of <140 Å²³⁶. Molecules that obey the restrictions are more likely to show preferable membrane permeability. To this end, molecular properties of the studied compounds were calculated (Table 1).

Properties calculated using QikProp software (Schrödinger Ltd): QLogP – Predicted octanol/water partition coefficient; MW – molecular weight; HBD – hydrogen bond donor; HBA – hydrogen bond acceptor; RB – rotatable bonds; TPSA – total polar surface area (Å²). Number of PAINS alerts reported by SwissADME.

The novel compounds comply with Lipinski and Veber rules and may be therefore considered drug-like. The determined crucial molecular properties show high probability that the molecules will be bioavailable *per os*. Moreover, the designed structures were examined for known classes of reactive assay interference compounds that would disturb biological *in vitro* studies. According to SwissADME tool³¹, none of the compounds contain substructural features recognized as pan assay interference compounds (PAINS) (Table 1).

To further characterize the designed molecules, important ADME parameters were predicted. The compounds were characterized by moderate to high predicted water solubility (20–1259 µM/L,



Scheme 1. Synthesis of compounds **3–11**. Reagents and conditions: (a) TEA, K₂CO₃, acetone, reflux, 72 h, 60%; Method b: corresponding arylpiperazine, KI, K₂CO₃, dioxane, reflux, 72 h; Method c: corresponding arylpiperazine, 140 °C, 30 min. Demethylation of **6**: BBr₃, DCM, 0 °C, 24 h.

Table 2. Predicted ADME parameters.

Compound	QLogS	QPPCaco [nm/s]	PO [%]	BBB	Pgp	PB [%]	MetStab [%]
3	−4.5	927	100	Yes	No	87	29
4	−4.7	850	100	Yes	No	100	23
5	−6.0	676	94	Yes	No	92	19
6	−4.2	688	100	Yes	No	88	27
7	−4.2	231	89	Yes	Yes	84	36
8	−2.9	486	91	No	Yes	69	45
9	−4.7	707	100	Yes	Yes	90	16
10	−3.3	122	78	No	Yes	81	42
11	−4.4	120	80	No	Yes	84	36

Table 3. Functional activity results for compounds **3–11**. Antagonist potency towards alpha 2B-AR, expressed as IC₅₀ (nM) ± SEM values

Compound	Antagonist mode (IC ₅₀ ± SEM) [nM]
3	61 ± 25.4
4	251 ± 71
5	>1000
6	>1000
7	758 ± 160
8	>1000
9	47 ± 12.8
10	61 ± 22.5
11	>1000
ARC-239	8.4 ± 3.2

expect of compound **5** – 1 µM/L), which together with fair predicted Caco-2 cells permeability (compounds having permeability values over 500 nm/s are considered well-permeable through gut-blood barrier) stands for their favorable predicted human oral absorption (78–100%). Majority of the compounds (except compounds **8**, **10**, and **11**) were predicted to have the ability to cross the blood-brain-barrier (BBB). It has been suggested that anti-coagulant activity in central nervous system might be regarded as potential prevention of brain stroke, thus the ability of designed compound to cross the blood-brain-barrier in this aspect might be beneficial³⁷. Moreover, compounds **3–6** are not supposed to be P-gp substrates. The tested compounds are expected to bind with serum albumins at the rate of 69–100% and are supposed to have fair metabolic stability after CYP3A4 incubation (16–45% compound remaining, while compounds having predicted over 50% are considered metabolically stable) (Table 2).

Predicted parameters: QLogS – solubility; QPPCaco – Caco-2 cell permeability; %PO Absorption – percent human oral absorption (QikProp, Schrödinger Ltd.); BBB – blood-brain-barrier permeability; Pgp – substrate of glycoprotein P (SwissADME); PB – % of protein binding; MetStab – metabolic stability after CYP incubation (VolSurf+, Molecular Discovery).

In vitro assays

Considering that a potent blockade of alpha 2B-ARs is required for the antiplatelet effect^{8,9} we began an assessment of a pharmacological profile of all the synthesized molecules (**3–11**) with the evaluation of their alpha 2B-ARs antagonistic properties. The majority of the final molecules (**3**, **4**, **9**, and **10**) elicited a potent blockade of the alpha 2B-ARs, with the IC₅₀ values ranging from 47 to 251 nM (Table 3). Next, we have determined the selectivity of the obtained compounds vs. alpha 2A-adrenoreceptor subtype. All of the molecules showed a negligible affinity for alpha-2A adrenoreceptor giving no significant effect at the concentration of 1.0E−05 M. The above results suggest the desired level of selectivity vs. alpha 2A-AR subtype.

Table 4. The results of binding to alpha1-AR of the final compounds **3–11** and the reference ARC-239 expressed as K_i ± SD values.

Compound	Affinity for alpha 1-ARs K _i ± SD [nM]
3	30.0 ± 1.0
4	93.0 ± 2.0
5	703 ± 1
6	78.4 ± 3.8
7	81.70 ± 5.5
8	1500.0 ± 100.0
9	30 ± 0.2
10	10.3 ± 0.3
11	3.0 ± 0.1
ARC-239	0.3

Subsequently, we determined the selectivity vs. alpha 1-adrenoreceptor (Table 4). The final compounds **3–11** were submitted to a radioligand binding assay, measuring the ability to displace [³H] prazosin from alpha 1-ARs, in the rat cerebral cortex. ARC-239 was used as a reference and it showed high binding properties for alpha 1-ARs, with the K_i value of 0.3 nM. These results are with the agreement with the previous reports^{13,15}. The majority of newly synthesized compounds showed a weaker affinity for alpha 1-ARs comparing to ARC-239. It was found that the replacement of 2-methoxybenzene group with pyrimidine ring caused the most significant drop in alpha1-AR affinity. On the other hand, the introduction of a hydrophobic group into meta position of the phenylpiperazine ring (**3**, **4**, **5**, **6**) caused a relatively weaker decrease. Interestingly, incorporation of hydroxyl group into meta position of the phenylpiperazine ring gave similar result and caused slight decrease in affinity. The incorporation of a bulky substituents such as; 2,2-dimethylbenzo[d][1,3]dioxole (**9**), benzo[d]oxazol-2(3H)-one (**10**), 2H-benzo[b][1,4]oxazin-3(4H)-one (**11**) maintained the affinity for alpha1-ARs. However, the K_i (3–30 nM) values were still significantly higher than for ARC-239. The results of structure-activity relationship unambiguously showed that the introduced modifications maintained antagonistic activity at alpha 2B-AR, did not increase the affinity for alpha 2A-AR and reduced the affinity for alpha 1-AR.

Based on the aforementioned results, the most interesting compounds (**3**, **4**, **9**, and **10**) were selected for further studies. In order to evaluate the anti-platelet effects of the new compounds *in vitro*, freshly isolated rat whole blood was incubated with selected compounds (3–100 µM) or vehicle (DMSO), and the aggregation responses were evaluated with multiplate whole blood aggregometer by measuring impedance change. Platelet aggregation was induced by collagen or sub-threshold concentration of ADP and adrenaline. ARC-239 was used as a reference compound.

Compounds **3**, **4**, **9**, and **10** were found to inhibit collagen-induced platelet aggregation *in vitro* as presented in Figure 3 and Table 3. Compound **9** was active at the concentration of 100 µM, attenuating platelet aggregation to 59.3%. Compounds **3**, **4**, and **9** exhibited significant anti-platelet efficacies also at lower concentration (30 µM) giving IC₅₀ values ranging from 26.9 ± 2.5 µM³ to 34.5 ± 18.8 µM⁴. The IC₅₀ value for ARC-239 was in the similar range as for the studied compounds and was equal to 20.7 ± 14.7 µM.

Further studies showed that three compounds: **3**, **9**, and **10** also inhibited aggregation induced by the sub-threshold concentration of ADP and adrenaline. At a concentration of 1.6 µM, ADP alone, only partially and transiently aggregated rat blood *in vitro*, whereas adrenaline alone did not cause aggregation at any concentration tested. Combining adrenaline with the sub-threshold concentration of ADP produced a maximal aggregation response.

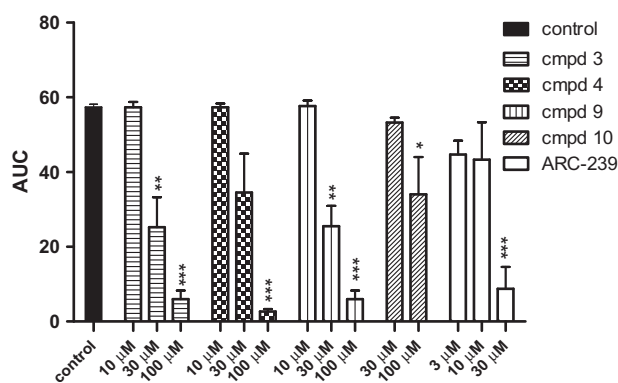


Figure 3. Effects of the studied compounds and ARC-239 on *in vitro* whole rat blood aggregation induced by collagen (1.6 µg/mL). Results are expressed as mean ± SEM, $n=3-6$, * $p < .05$, ** $p < .01$, *** $p < .001$ vs. control group (0.1% DMSO in saline).

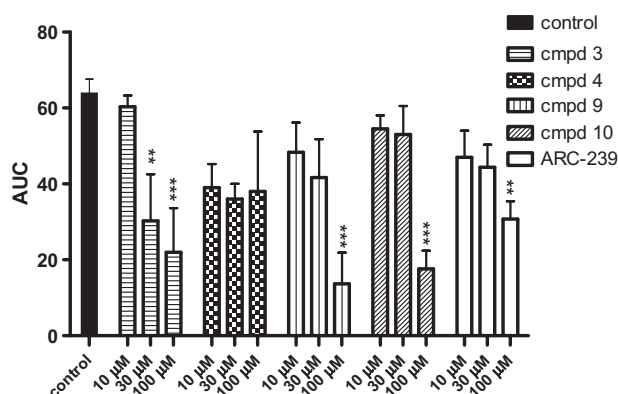


Figure 4. Effects of studied compounds and ARC-239 on *in vitro* whole rat blood aggregation induced by simultaneous addition of adrenaline and ADP (50 µM + 1.6 µM). Results are expressed as mean ± SEM, $n=3-9$, ** $p < .01$, *** $p < .001$ versus control group (0.1% DMSO in saline).

Table 5. Potencies of the studied compounds and ARC-239 in inhibition *in vitro* whole rat blood aggregation induced by (A) collagen (1.6 µg/mL), (B) ADP and adrenaline (1.6 µM + 50 µM).

Compound	A (collagen) IC ₅₀ [µM]	B (ADP + A) IC ₅₀ [µM]
3	26.9 ± 18.8	20.5 ± 7.1
4	34.5 ± 2.5	n.a.
9	27.4 ± 5.3	54.4 ± 5.4
10	n.a.	76.5 ± 5.8
ARC-239	20.7 ± 14.7	63.9 ± 21.3

IC₅₀ (concentration of the compound that inhibits the whole rat blood aggregation *in vitro* by 50%), n.a. – not active.

Table 6. *In vitro* bioavailability data for compound 3.

Assay	Test Concentration [M]	Property
Aqueous solubility (simulated intestinal fluid)	2.0E-04	Solubility [µM]
Aqueous solubility (PBS, pH 7.4)		68.0
Aqueous solubility (simulated gastric fluid)		5.4
		150.9
Protein binding (plasma, human)	1.0E-05	% Protein bound
		99
A-B permeability (Caco-2, pH 6.5/7.4)	1.0E-05	Permeability [10 ⁻⁶ cm/s]
B-A permeability (Caco-2, pH 6.5/7.4)		7.7
		2.6
	Incubation time [minutes]	% Compound remaining
		Half-life [minute]
		Intrinsic clearance [µL/min/mg]
Metabolic stability (liver microsomes, human)	1.0E-07	14.1
	0	100.0
	15	49
	30	18
	45	8
	60	6

The adrenaline-mediated amplification of ADP-stimulated aggregation was attenuated when rat blood was pre-incubated with **3**, **9**, **10**, and ARC-239. The IC₅₀ values ranged from 20.5 µM³ to 76.5 µM¹⁰. The IC₅₀ value for ARC-239 was in the similar range as for the studied compounds **9** and **10** and it was equal to 63.9 ± 21.3 µM. Compound **4**, even up to 100 µM, did not exhibit any significant inhibition against ADP and adrenaline induced blood aggregation. The results are presented in Figure 4 and Table 5. Compound **3** was observed to be the most potent among the entire series and exhibited an IC₅₀ of 26.9 µM against collagen and 20.5 µM against ADP and adrenaline induced blood aggregation and **3** was also superior to ARC-239 concerning ADP-adrenaline induced aggregation.

Concerning the described above results, for the most promising compound **3**, we performed early *in vitro* bioavailability assays, including aqueous solubility, human plasma protein binding, human liver microsomes stability, and Caco-2 permeability (Eurofins Bioavailability panel). The results are summarized in Table 6.

Compound **3** displayed moderate aqueous solubility (in PBS pH 7.4 = 5.4 µM, simulated gastric fluid = 150.9 µM and simulated intestinal fluid = 68.0 µM), high plasma protein binding (99%), fair metabolic stability (half-life 14.1 min, intrinsic clearance 14 ml/min/mg), and fair Caco-2 permeability (7.7 × 10⁻⁶ cm/s). Such characteristics leave space for further optimization; however, they support the selection of compound **3** for subsequent *in vivo* studies, that will be addressed in the future.

Conclusions

In summary, we have synthesized a series of *N*-arylpiperazine derivatives of 4,4-dimethylisoquinoline-1,3(2*H*,4*H*)-dione as potent alpha 2B-receptor antagonists. The compounds were generated by changing the substitution pattern at the phenylpiperazine moiety of a known alpha 2B ARs antagonist, compound ARC-239, which also exhibits a strong binding affinity for alpha 1 AR receptors. The applied modification maintained an antagonistic activity at alpha 2B-ARs and reduced the affinity for alpha 1-ARs. The anti-platelet effects of the new compounds were evaluated in *in vitro* models. The most potent analog among all the series was compound **3**, since it effectively inhibited the platelet-aggregation induced both by collagen and ADP/adrenaline. At the same time, compound **3** displayed drug-like properties in computational predictions, which were positively verified by *in vitro* bioavailability assays. The results of our study confirm that the alpha 2B-AR antagonists remain an

interesting target for the development of novel antiplatelet agents with a different mechanism of action. Further studies to extend the pharmacological profile of obtained compounds will be conducted.

Acknowledgements

The National Science Centre in Poland on the basis of the decision to issue DEC-2011/03/B/NZ7/00635 funded this project. Title of the grant: "Partial agonists of alpha-2 adrenoceptors as a new perspective of the effective and safe in reducing body weight and obesity".

Disclosure statement

No potential conflict of interest was reported by the authors.

Funding

This work was supported by The National Science Centre in Poland under Grant number DEC-2011/03/B/NZ7/00635; Uniwersytet Jagielloński Collegium Medicum under Grant number K/ZDS/006235.

References

- Vos CG, Vahl A. Anticoagulation and antiplatelet therapy in patients with peripheral arterial disease of the femoro-popliteal arteries. *J Cardiovasc Surg (Torino)* 2017. [Epub ahead of print]. doi: [10.23736/S0021-9509.17.10210-7](https://doi.org/10.23736/S0021-9509.17.10210-7)
- Bezin J, Klungel OH, Lassalle R, et al. Medications recommended for secondary prevention after first acute coronary syndrome: effectiveness of treatment combinations in a real-life setting. *Clin Pharmacol Ther* 2017. [Epub ahead of print]. doi: [10.1002/cpt.864](https://doi.org/10.1002/cpt.864)
- Shrestha S, Coy S, Bekelis K. Oral antiplatelet and anticoagulant agents in the prevention and management of ischemic stroke. *Curr Pharm Des* 2017;23:1377–91.
- Angiolillo DJ. Antiplatelet therapy in diabetes: efficacy and limitations of current treatment strategies and future directions. *Diabetes Care* 2009;32:531–40.
- Lev EI, Patel RT, Maresh KJ, et al. Aspirin and clopidogrel drug response in patients undergoing percutaneous coronary intervention: the role of dual drug resistance. *J Am Coll Cardiol* 2006;47:27–33.
- Nordeen JD, Patel AV, Darracott RM, et al. Clopidogrel resistance by P2Y₁₂ platelet function testing in patients undergoing neuroendovascular procedures: incidence of ischemic and hemorrhagic complications. *J Vasc Interv Neurol* 2013;6:26–34.
- Béres BJ, Tóth-Zsámboki E, Vargová K, et al. Analysis of platelet alpha₂-adrenergic receptor activity in stable coronary artery disease patients on dual antiplatelet therapy. *Thromb Haemost* 2008;100:829–38.
- Marketou ME, Kintsurashvili E, Androulakis NE, et al. Blockade of platelet alpha_{2B}-adrenergic receptors: a novel antiaggregant mechanism. *Int J Cardiol* 2013;168:2561–6.
- Marketou M, Kochiadakis G, Kintsurashvili E, et al. Blockade of platelet alpha_{2B}-adrenergic receptors in patients with coronary artery disease: a novel antiaggregant mechanism. *Eur Heart J* 2013;34(suppl 1):574. doi: [10.1093/eurheartj/eh309.P3138](https://doi.org/10.1093/eurheartj/eh309.P3138)
- Goto S, Ikeda Y, Murata M, et al. Epinephrine augments von Willebrand factor-dependent shear-induced platelet aggregation. *Circulation* 1992;86:1859–63.
- Mustonen P, Lassila R. Epinephrine augments platelet recruitment to immobilized collagen in flowing blood—evidence for a von Willebrand factor-mediated mechanism. *Thromb Haemost* 1996;75:175–81.
- Menziani MC, Montorsi M, De Benedetti PG, Karelson M. Relevance of theoretical molecular descriptors in quantitative structure-activity relationship analysis of alpha₁-adrenergic receptor antagonists. *Bioorg Med Chem* 1999;7:2437–51.
- Wang CD, Buck MA, Fraser CM. Site-directed mutagenesis of alpha_{2A}-adrenergic receptors: identification of amino acids involved in ligand binding and receptor activation by agonists. *Mol Pharmacol* 1991;40:168–79.
- Rosenbaum DM, Rasmussen SGF, Kobilka BK. The structure and function of G-protein-coupled receptors. *Nature* 2009;459:356–63.
- Bylund DB, Ray-Prenger C, Murphy TJ. Alpha-2A and alpha-2B adrenergic receptor subtypes: antagonist binding in tissues and cell lines containing only one subtype. *J Pharmacol Exp Ther* 1988;245:600–7.
- Li M-Y, Tsai K-C, Xia L. Pharmacophore identification of alpha_{1A}-adrenoceptor antagonists. *Bioorg Med Chem Lett* 2005;15:657–64.
- Carruthers SG. Adverse effects of alpha₁-adrenergic blocking drugs. *Drug Saf* 1994;11:12–20.
- Waszkielewicz AM, Kubacka M, Pańczyk K, et al. Synthesis and activity of newly designed aroxyalkyl or aroxyethoxyethyl derivatives of piperazine on the cardiovascular and the central nervous systems. *Bioorg Med Chem Lett* 2016;26:5315–21.
- Bednarski M, Otto M, Dudek M, et al. Synthesis and pharmacological activity of a new series of 1-(1H-indol-4-yloxy)-3-(2-(2-methoxyphenoxy)ethylamino)propan-2-ol analogs. *Arch Pharm (Weinheim)* 2016;349:211–23.
- Lopez-Rodriguez ML, Ayala D, Benhamu B, et al. Arylpiperazine derivatives acting at 5-HT_{1A} receptors 5. *Curr Med Chem* 2002;9:443–69.
- Huff JR, Baldwin JJ, deSolms SJ, et al. Structure-affinity relationships of arylquinolizines at alpha-adrenoceptors. *J Med Chem* 1988;31:641–5.
- Cockroft SL, Perkins J, Zonta C, et al. Substituent effects on aromatic stacking interactions. *Org Biomol Chem* 2007;5:1062–80.
- Lopez-Rodriguez ML, Morcillo MJ, Fernandez E, et al. Synthesis and structure-activity relationships of a new model of arylpiperazines. 5.(1) Study of the physicochemical influence of the pharmacophore on 5-HT_{1A}/alpha₁-adrenergic receptor affinity: synthesis of a new derivative with mixed 5-HT_{1A}/D(2) antagonist properties. *J Med Chem* 2001;44:186–97.
- Lopez-Rodriguez ML, Morcillo MJ, Fernandez E, et al. Synthesis and structure-activity relationships of a new model of arylpiperazines. 8. Computational simulation of ligand-receptor interaction of 5-HT_{1A} agonists with selectivity over alpha₁-adrenoceptors. *J Med Chem* 2005;48:2548–58.
- Ostopovici-Halip L, Curpăn R, Mracec M, Bologa CG. Structural determinants of the alpha₂ adrenoceptor subtype selectivity. *J Mol Graph Model* 2011;29:1030–8.
- Xhaard H, Nyrönen T, Rantanen V-V, et al. Model structures of α -2 adrenoceptors in complex with automatically docked antagonist ligands raise the possibility of interactions dissimilar from agonist ligands. *J Struct Biol* 2005;150:126–43.

27. Kołaczowski M, Bucki A, Feder M, Pawłowski M. Ligand-optimized homology models of D1 and D2 dopamine receptors: application for virtual screening. *J Chem Inf Model* 2013;53:638–48.
28. Cherezov V, Rosenbaum DM, Hanson MA, et al. High-resolution crystal structure of an engineered human beta2-adrenergic G protein-coupled receptor. *Science* 2007;318:1258–65.
29. Kurowski MA, Bujnicki JM. GeneSilico protein structure prediction meta-server. *Nucleic Acids Res* 2003;31:3305–7.
30. Arnold K, Bordoli L, Kopp J, Schwede T. The SWISS-MODEL workspace: a web-based environment for protein structure homology modelling. *Bioinforma Oxf Engl* 2006;22:195–201.
31. Daina A, Michielin O, Zoete V. SwissADME: a free web tool to evaluate pharmacokinetics, drug-likeness and medicinal chemistry friendliness of small molecules. *Sci Rep* 2017;7:42717.
32. Lipinski CA, Lombardo F, Dominy BW, Feeney PJ. Experimental and computational approaches to estimate solubility and permeability in drug discovery and development settings. *Adv Drug Deliv Rev* 2001;46:3–26.
33. Banker MJ, Clark TH, Williams JA. Development and validation of a 96-well equilibrium dialysis apparatus for measuring plasma protein binding. *J Pharm Sci* 2003;92:967–74.
34. Borchardt RT, Hidalgo IJ, Raub TJ, Borchardt RT. Characterization of the human colon carcinoma cell line (Caco-2) as a model system for intestinal epithelial permeability, *Gastroenterology*, 96, 736–749, 1989—the backstory. *AAPS J* 2011;13:323–7.
35. Obach RS, Baxter JG, Liston TE, et al. The prediction of human pharmacokinetic parameters from preclinical and in vitro metabolism data. *J Pharmacol Exp Ther* 1997;283:46–58.
36. Veber DF, Johnson SR, Cheng H-Y, et al. Molecular properties that influence the oral bioavailability of drug candidates. *J Med Chem* 2002;45:2615–23.
37. Shahpoury MM, Mousavi S, Khorvash F, et al. Anticoagulant therapy for ischemic stroke: a review of literature. *J Res Med Sci off J Isfahan Univ Med Sci* 2012;17:396–401.